organic compounds

Hydrogen-bonding patterns in 3-alkyl-3-hydroxyindolin-2-ones

Diana Becerra,[a] Braulio Insuasty,[a] Justo Cobo[b] and Christopher Glidewell[c]*

[a]Departamento de Química, Universidad de Valle, AA 25360 Cali, Colombia, [b]Departamento de Química Inorgánica y Orgánica, Universidad de Jaén, 23071 Jaén, Spain, and [c]School of Chemistry, University of St Andrews, Fife KY16 9ST, Scotland

Correspondence e-mail: cg@st-andrews.ac.uk

The molecules of racemic 3-benzoylmethyl-3-hydroxyindolin-2-one, $C_{16}H_{13}NO_3$, (I), are linked by a combination of N—H⋯O and O—H⋯O hydrogen bonds into a chain of centrosymmetric edge-fused $R_2^2(10)$ and $R_4^4(12)$ rings. Five monosubstituted analogues of (I), namely racemic 3-hydroxy-3-[(4-methylbenzoyl)methyl]indolin-2-one, $C_{17}H_{15}NO_3$, (II), racemic 3-[(4-fluorobenzoyl)methyl]-3-hydroxyindolin-2-one, $C_{16}H_{12}FNO_3$, (III), racemic 3-[(4-chlorobenzoyl)methyl]-3-hydroxyindolin-2-one, $C_{16}H_{12}ClNO_3$, (IV), racemic 3-[(4-bromobenzoyl)methyl]-3-hydroxyindolin-2-one, $C_{16}H_{12}BrNO_3$, (V), and racemic 3-hydroxy-3-[(4-nitrobenzoyl)methyl]-indolin-2-one, $C_{16}H_{12}N_2O_5$, (VI), are isomorphous in space group $P\bar{1}$. In each of compounds (II)–(VI), a combination of N—H⋯O and O—H⋯O hydrogen bonds generates a chain of centrosymmetric edge-fused $R_2^2(8)$ and $R_2^2(10)$ rings, and these chains are linked into sheets by an aromatic π–π stacking interaction. No two of the structures of (II)–(VI) exhibit the same combination of weak hydrogen bonds of C—H⋯O and C—H⋯π(arene) types. The molecules of racemic 3-hydroxy-3-(2-thienylcarbonylmethyl)indolin-2-one, $C_{14}H_{11}NO_3S$, (VII), form hydrogen-bonded chains very similar to those in (II)–(VI), but here the sheet formation depends upon a weak π–π stacking interaction between thienyl rings. Comparisons are drawn between the crystal structures of compounds (I)–(VII) and those of some recently reported analogues having no aromatic group in the side chain.

Comment

We report here the structures of seven racemic 3-hydroxy-3-(2-aryl-2-oxoethyl)indolin-2-ones, *viz.* compounds (I)–(VII) (Fig. 1), which we compare with the structures of a number of analogues, (VIII)–(XII), in the recent literature (Luppi *et al.*, 2005, 2006; Xing *et al.*, 2007; Chen *et al.*, 2009). Chalcones are versatile bis-electrophilic reagents widely employed in the synthesis of fused heterocyclic systems, and compounds (I)–

(VII) have been prepared as precursors for the formation of chalcones by acid-catalysed dehydration reactions.

(I) X = H
(II) X = CH₃
(III) X = F
(IV) X = Cl
(V) X = Br
(VI) X = NO₂
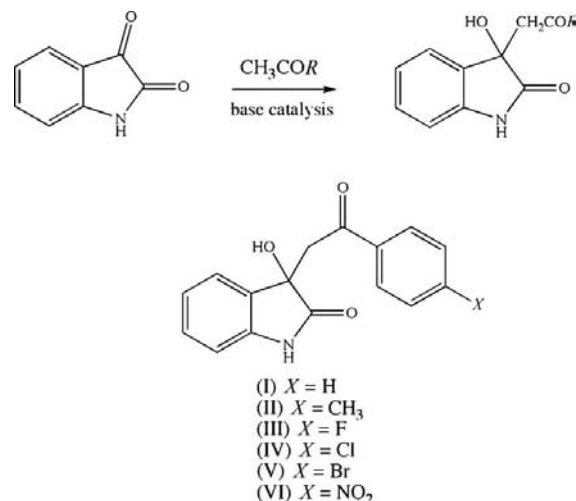
Compounds (I)–(VII) were prepared by reactions of isatin with methyl ketones using basic catalysis (see scheme), as were the analogues (VIII)–(XII). The compounds all contain a stereogenic centre, at atom C3 in (I)–(VII) (Fig. 1), and if an achiral base is employed as the catalytic agent, as here, the products are obtained as racemic mixtures. However, if an enantiomerically pure form of a chiral base is used, then the products are found with a significant excess of one enantiomer over the other, as in the syntheses of (IX) (Luppi *et al.*, 2005), (XI) (Luppi *et al.*, 2006) and (XII) (Xing *et al.*, 2007).

(VII)

(VIII), MUBMAY

(IX), TAWDUR

(X), TAWFAZ

(XI), TEQVUH

(XII), YIZFIX
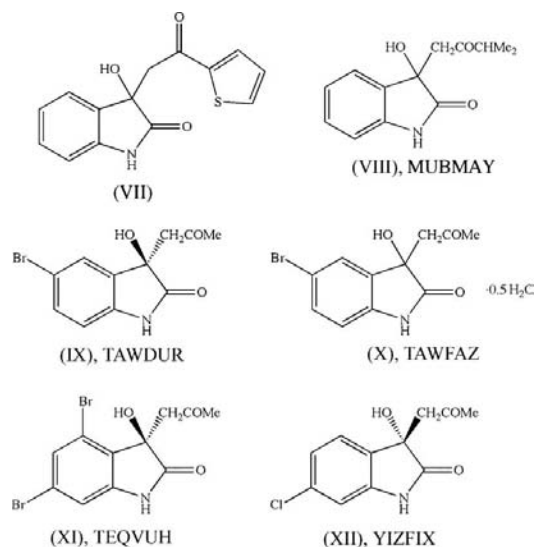
As expected from the method of synthesis, (I)–(VII) all crystallize as racemic mixtures and all crystallize in centrosymmetric space groups. However, while compound (I), which contains an unsubstituted phenyl ring in the side chain (Fig. 1a), crystallizes in the space group $P2_1/c$, compounds (II)–(VI), which all contain a single substituent at the 4-position of this ring (Fig. 1b–1f), are all isomorphous in the space group $P\bar{1}$. Compound (VII), which contains a 2-thienyl unit rather than an aryl ring in the side chain (Fig. 1g), also crystallizes in the space group $P\bar{1}$ and the unit-cell repeat
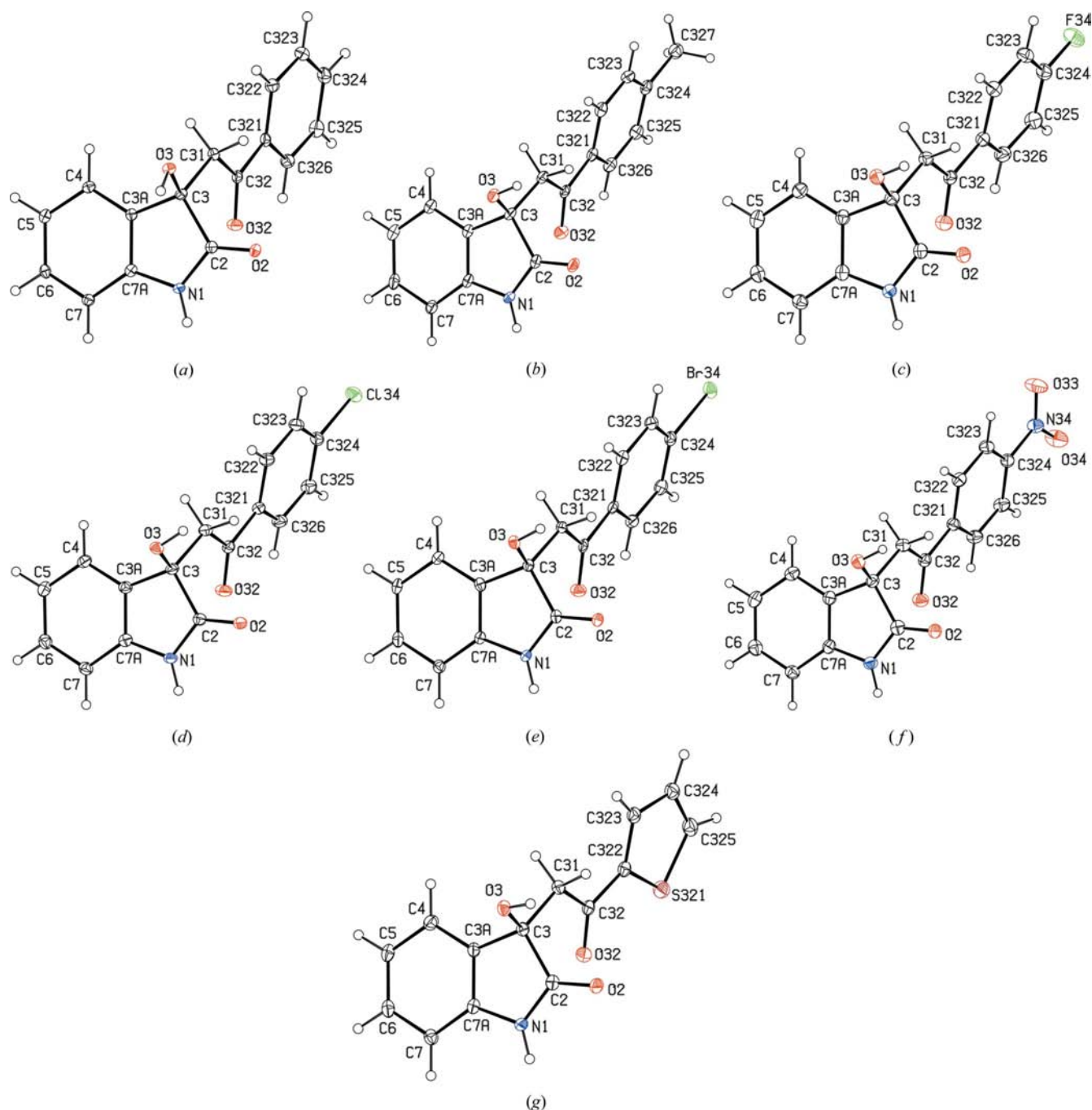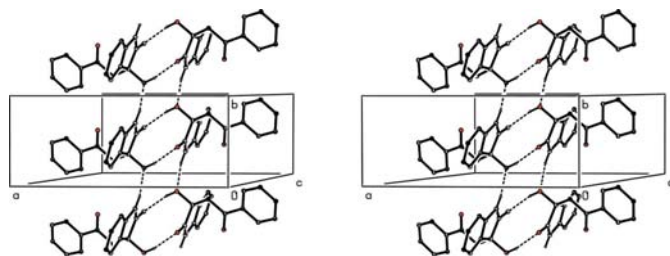
Figure 1
The molecular structures and atom-labelling schemes for (a) (I), (b) (II), (c) (III), (d) (IV), (e) (V), (f) (VI) and (g) (VII). Displacement ellipsoids are drawn at the 30% probability level and H atoms are shown as small spheres of arbitrary radii.

distances a, b and c are similar to those in compounds (II)–(VI). The unit-cell angles have approximately complementary values to those in (II)–(VI) and the atom coordinates in (VII) are approximately related to those of the corresponding atoms in (II)–(VI) by the transformation $(1 - x, y, 1 - z)$. However, comparison of the reduced-cell parameters shows that, despite these similarities, compound (VII) is not isomorphous with the series (II)–(VI).

In the crystal structure of (I), molecules related by translation are linked by an N—H···O hydrogen bond (Table 1) to form a $C(5)$ (Bernstein et al., 1995) chain running parallel to

the [010] direction. Antiparallel pairs of such chains are linked by an O—H···O hydrogen bond to generate a chain of centrosymmetric edge-fused rings, in which $R_2^2(10)$ rings centred at $(\frac{1}{2}, n + \frac{1}{2}, \frac{1}{2})$, where n represents an integer, alternate with $R_4^4(12)$ rings centred at $(\frac{1}{2}, n, \frac{1}{2})$, where n again represents an integer (Fig. 2). Two chains of this type pass through each unit cell but there are no direction-specific interactions of structural significance between adjacent chains.

Although compounds (II)–(VI) are isomorphous, they are not strictly isostructural (Acosta et al., 2009), as the pattern of the weaker hydrogen bonds of C—H···O and C—H···

Figure 2
A stereoview of part of the crystal structure of (I), showing the formation of a hydrogen-bonded chain of alternating $R_2^2(10)$ and $R_4^4(12)$ rings along [100]. Hydrogen bonds are shown as dashed lines. For the sake of clarity, H atoms bonded to C atoms have been omitted.
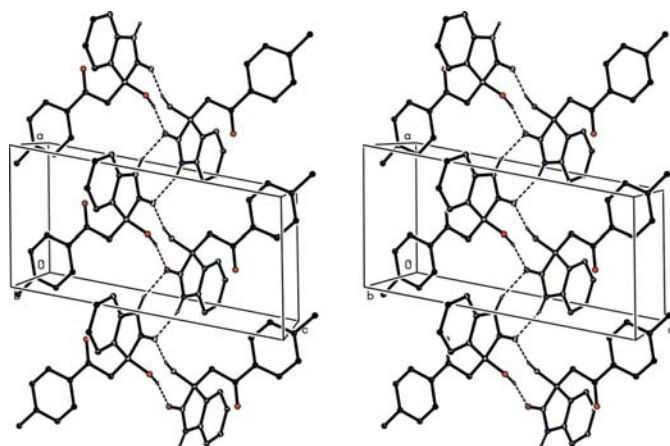
Figure 3
A stereoview of part of the crystal structure of (II), showing the formation of a hydrogen-bonded chain of alternating $R_2^2(8)$ and $R_2^2(10)$ rings along [100]. Hydrogen bonds are shown as dashed lines. For the sake of clarity, H atoms bonded to C atoms have been omitted.
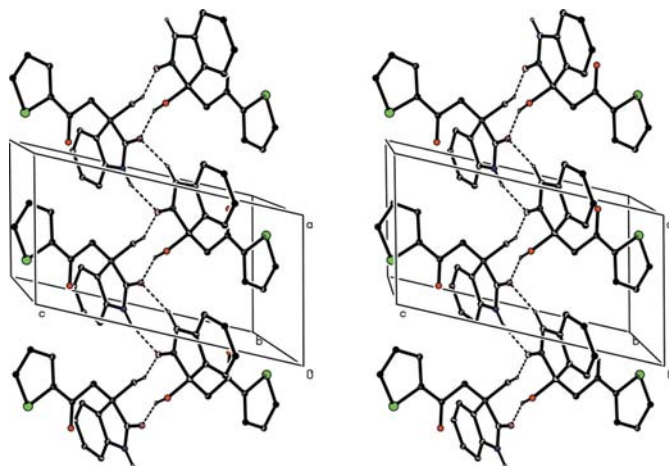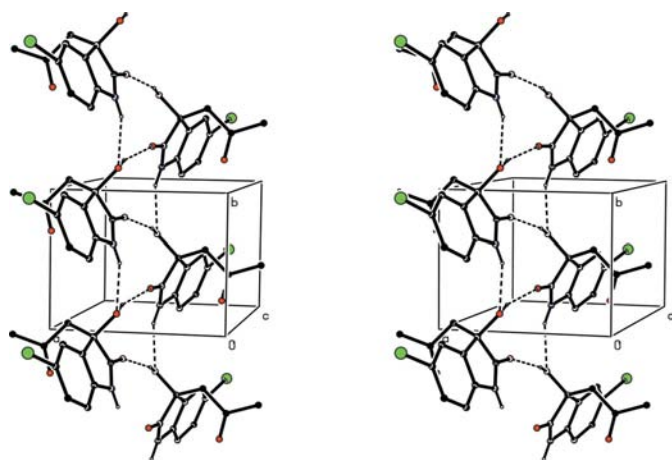

Figure 4
A stereoview of part of the crystal structure of (VII), showing the formation of a hydrogen-bonded chain of alternating $R_2^2(8)$ and $R_2^2(10)$ rings along [100]. Hydrogen bonds are shown as dashed lines. For the sake of clarity, H atoms bonded to C atoms have been omitted. Note the orientations of the unit cell and the chain relative to those in Fig. 3.

π(arene) types differs between the members of the series, such that no two of (II)–(VI) show an identical array of such interactions. Indeed, no interactions of these types occur in the structure of (II), while some of them are present in the structures of each of (III)–(VI). It is thus convenient to describe first the actions of the N—H$\cdots$O and O—H$\cdots$O hydrogen bonds and the aromatic π–π stacking interactions in compound (II), which are in fact the same in each of (II)–(VI), and then briefly to note the actions of the weaker hydrogen bonds in each of (III)–(VI).

In compound (II), symmetry-related pairs of O—H$\cdots$O hydrogen bonds (Table 1) link the molecules at (x, y, z) and $(1 - x, 1 - y, 1 - z)$ to form an $R_2^2(10)$ motif, while similar pairs of N—H$\cdots$O hydrogen bonds link the molecules at (x, y, z) and $(-x, 1 - y, 1 - z)$ to form an $R_2^2(8)$ motif. Propagation by inversion of these two motifs then generates a chain of edge-fused rings running parallel to the [100] direction, in which the $R_2^2(10)$ rings are centred at $(n + \frac{1}{2}, \frac{1}{2}, \frac{1}{2})$ and the $R_2^2(8)$ rings are centred at $(n, \frac{1}{2}, \frac{1}{2})$, where in both cases n represents an integer (Fig. 3). This chain of rings differs from that formed by (I) in two important respects. Firstly, both hydrogen bonds in (II) utilize amidic atom O2 as the acceptor, whereas in (I) the N—H$\cdots$O hydrogen bond utilizes hydroxy atom O3 as the acceptor. Secondly, the chain in (II) is

propagated solely by inversion, while a combination of translation and inversion propagates the chain in (I). However, one feature in common between these two chains is that in neither type does ketonic atom O32 in the side chain participate in the N—H$\cdots$O or O—H$\cdots$O hydrogen bonds. The hydrogen-bonded chains in (II) are linked by a single aromatic π–π stacking interaction involving the C321–C326 phenyl rings in the molecules at (x, y, z) and $(2 - x, 1 - y, 2 - z)$ (Table 2). These two molecules form parts of the hydrogen-bonded chains along $(x, \frac{1}{2}, \frac{1}{2})$ and $(x, \frac{1}{2}, \frac{3}{2})$, respectively, so that propagation of this π–π stacking interaction links the hydrogen-bonded chains into a sheet parallel to (010).

The formation of hydrogen-bonded [100] chains containing alternating $R_2^2(8)$ and $R_2^2(10)$ rings and linked by a π–π stacking interaction into sheets parallel to (010) is common to each of (II)–(VI) (Tables 1 and 2), and the sheet formation provides another point of difference between the crystal structures of (II)–(VI) on the one hand and that of (I) on the other. However, the structures of each of (III)–(VI) exhibit further weak interactions, different in each case, and thus different from the structure of (II). In each of (IV), (V) and (VI), although not in (II) or (III), there are C—H$\cdots$O hydrogen bonds which reinforce, albeit weakly, the chains along [100], and in each of (III) and (IV), but not in (II), (V) or (VI), there is a C—H$\cdots$$\pi$(arene) hydrogen bond which reinforces the linkage of the [100] chains into sheets. Although the structures of both (V) and (VI) contain C—H$\cdots$O hydrogen bonds, the number of these interactions differs in the two structures (Table 1). In addition, it may be noted that ketonic atom O32 is involved only in C—H$\cdots$O interactions in compounds (IV), (V) and (VI), rather than in N—H$\cdots$O or O—H$\cdots$O hydrogen bonds. Similarly, the only interaction involving a nitro group O atom in (VI) is of C—H$\cdots$O type.

In compound (VII), a chain of edge-fused $R_2^2(8)$ and $R_2^2(10)$ rings along [100] is formed (Fig. 4), similar to those in (II)–
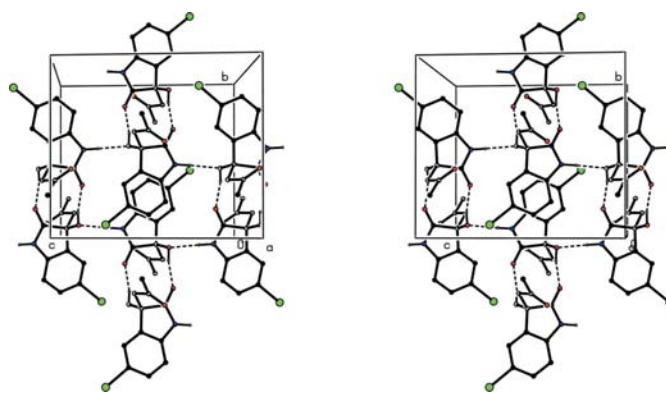
Figure 5
A stereoview of part of the crystal structure of (IX) (CSD refcode TAWDUR; Luppi *et al.*, 2005), showing the formation of a hydrogen-bonded chain of edge-fused $R_3^3(11)$ rings along [010]. Hydrogen bonds are shown as dashed lines. For the sake of clarity, H atoms bonded to C atoms have been omitted.
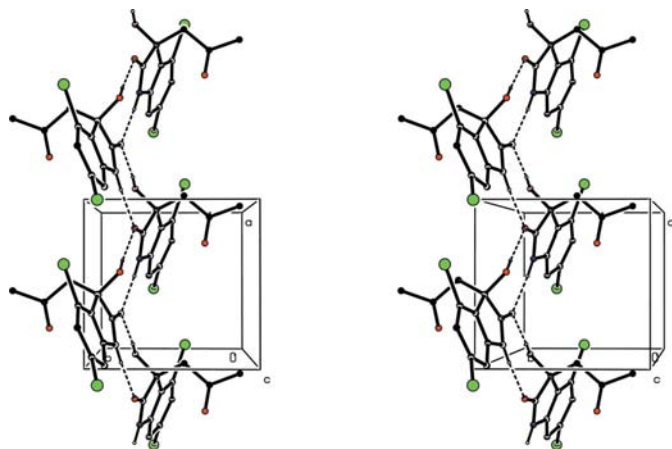

Figure 6
A stereoview of part of the crystal structure of (X) (CSD refcode TAWFAZ; Luppi *et al.*, 2005), showing the formation by the organic components of a hydrogen-bonded sheet parallel to (100) and containing $R_2^2(10)$ and $R_6^6(22)$ rings. Hydrogen bonds are shown as dashed lines. For the sake of clarity, H atoms bonded to C atoms have been omitted.

(VI), but the orientation of the hydrogen-bonded structure relative to the unit cell is different in (VII) from those in (II)–(VI) (Figs. 3 and 4). As with (IV)–(VI), the structure of (VII) contains two C—H$\cdots$O contacts within the hydrogen-bonded chains; these have rather long H$\cdots$O distances and only one of them involves hydroxy atom O3. However, the chains along [100] are again linked into sheets, this time rather weakly, by a π–π stacking interaction involving the thienyl rings of the molecules at (x, y, z) and $(1 - x, 1 - y, -z)$. These rings are strictly parallel, with an interplanar spacing of 3.368 (2) Å; the ring-centroid separation is 3.746 (2) Å, corresponding to a ring-centroid offset of 1.640 (2) Å. These two molecules are components of the hydrogen-bonded chains along $(x, \frac{1}{2}, \frac{1}{2})$ and $(x, \frac{1}{2}, -\frac{1}{2})$, respectively, so that this π–π stacking interaction links the hydrogen-bonded chains into a sheet parallel to (010), similar to those in (II)–(VI).

It is of interest to compare the structures of (I)–(VII) with those of some recently reported analogues, *viz.* (VIII)–(XII), several of which have been reported only briefly, usually on a simple proof-of-constitution or proof-of-configuration basis. Compounds (VIII)–(XII) differ from (I)–(VII) in several respects. Firstly, they have no aryl or heteroaryl group in the side chain, thus reducing the scope for the formation of C—H$\cdots$O and C—H$\cdots\pi$(arene) hydrogen bonds and of aromatic π–π stacking interactions. Secondly, compounds (IX), (XI) and (XII) crystallize in Sohncke space groups so that only a single enantiomer is present in a given crystal (provided that twinning is shown to be absent). Finally, compound (X) is a hemihydrate, while solvent molecules are not found in any other member of this series.

Compound (VIII) [Cambridge Structural Database (CSD; Allen, 2002) refcode MUBMAY; Chen *et al.*, 2009] crystallizes as a racemic mixture in the space group $P2_1/c$, and a combination of N—H$\cdots$O and O—H$\cdots$O hydrogen bonds generates a chain of alternating $R_2^2(10)$ and $R_4^4(12)$ rings propagated by translation and inversion along the [010] direction, entirely analogous to the chain in (I).

Compounds (IX) (CSD refcode TAWDUR; Luppi *et al.*, 2005) and (X) (CSD refcode TAWFAZ; Luppi *et al.*, 2005) were crystallized from the same solution following reaction of 5-bromoisatin with acetone catalysed by an enantiomerically pure D-prolyl dipeptide. Compound (XI) is the pure R enantiomer crystallizing in the space group $P2_1$, while (X) is a hemihydrate of the racemic mixture, which crystallizes in the space group $C2/c$. For (IX), the original report (Luppi *et al.*, 2005) indicated the formation of a hydrogen-bonded chain of rings, although without providing any details, but the structure of (X) was not mentioned at all. Re-examination of the structure of (IX) using the deposited atomic coordinates shows that molecules related by a 2_1 screw axis along $(\frac{1}{2}, y, 0)$ are linked by N—H$\cdots$O and O—H$\cdots$O hydrogen bonds to form a chain of edge-fused $R_3^3(11)$ rings (Fig. 5), with no direction-specific interactions between the chains.

Analysis of the structure of (X) using the deposited atomic coordinates shows that the hydrogen bonding links the molecular components into a three-dimensional framework structure, the formation of which is readily analysed in terms of the actions of the three hydrogen bonds in turn. Enantiomeric pairs of the organic component are linked by pairs of symmetry-related O—H$\cdots$O hydrogen bonds, forming centrosymmetric $R_2^2(10)$ dimers, analogous to those observed in (II)–(VIII). These dimers are linked by the N—H$\cdots$O hydrogen bond to form a sheet parallel to (100), containing both $R_2^2(10)$ and $R_6^6(22)$ rings and lying in the domain $(0 < x < \frac{1}{2})$ (Fig. 6). The water molecule lies on a twofold rotation axis along $(\frac{1}{2}, y, \frac{1}{4})$ and forms pairs of O—H$\cdots$O hydrogen bonds which link adjacent (100) sheets, so linking all of the molecules into a single three-dimensional structure.

The structure of the R enantiomer of (XI) (CSD refcode TEQVUH; Luppi *et al.*, 2006) was reported as a proof of constitution and configuration, as shown by the value, -0.006 (8), of the Flack x parameter (Flack, 1983), but no description or discussion of the crystal structure was given. This single enantiomer crystallizes in the space group $P2_12_12_1$ and examination of the crystal structure using the deposited
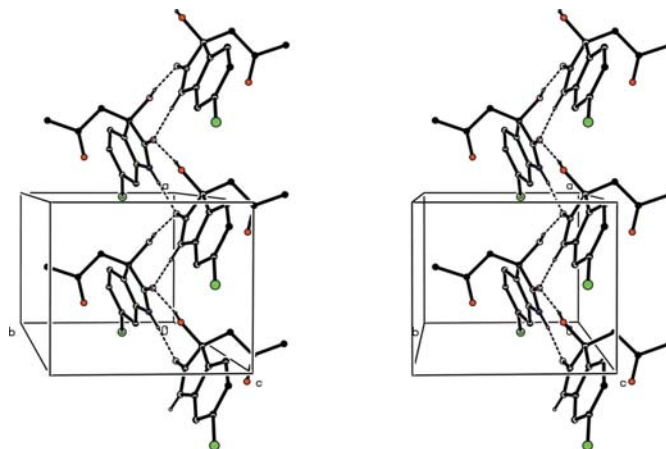
Figure 7
A stereoview of part of the crystal structure of (XI) (CSD refcode TEQVUH; Luppi *et al.*, 2006), showing the formation of a hydrogen-bonded chain of edge-fused $R_2^2(9)$ rings along [100]. Hydrogen bonds are shown as dashed lines. For the sake of clarity, H atoms bonded to C atoms have been omitted.

Figure 8
A stereoview of part of the crystal structure of (XII) (CSD refcode YIFZIX; Xing *et al.*, 2007), showing the formation of a hydrogen-bonded chain of edge-fused $R_2^2(9)$ rings along [100]. Hydrogen bonds are shown as dashed lines. For the sake of clarity, H atoms bonded to C atoms have been omitted.

atomic coordinates shows the formation of a chain of edge-fused $R_2^2(9)$ rings built from molecules related by the 2_1 screw axis along $(x, \frac{3}{4}, 1)$ and linked by N—H⋯O and O—H⋯O hydrogen bonds (Fig. 7).

Compound (XII) (CSD refcode YIFZIX; Xing *et al.*, 2007) also crystallizes in the space group $P2_12_12_1$ and the Flack x parameter of 0.03 (8) indicates that only a single enantiomer is present in the crystal selected for data collection. However, the identity of this enantiomer is nowhere specified in the original report, although the deposited coordinates correspond to the *S* enantiomer, consistent with the reported use of an L-prolyl amide as the catalytic base. The crystal structure was described as consisting of a chain of centrosymmetric $R_2^2(9)$ rings, but this description must be incorrect on two grounds, firstly because centrosymmetric motifs cannot contain an odd number of atoms, and secondly because centrosymmetric motifs cannot be formed in the noncentrosymmetric space group $P2_12_12_1$. The packing diagram provided by the authors does not show a chain. In fact, re-examination of this structure shows that it contains a chain of $R_2^2(9)$ rings entirely analogous to the chain in compound (XI), but built from molecules related by the 2_1 screw axis along $(x, \frac{1}{4}, \frac{1}{2})$ (Fig. 8).

In conclusion, compounds (I)–(XIII) discussed here exhibit several distinct patterns formed by conventional strong hydrogen bonds of N—H⋯O and O—H⋯O types. Thus, (I) and (VIII) form entirely similar hydrogen-bonded chains, despite the differences between the steric requirements of the terminal groups in their side chains, *viz.* phenyl in (I) and isopropyl in (VIII). A second pattern of chain formation is found in the isomorphous compounds (II)–(VI), as well as in (VII). A third type of chain formation is shared by the enantiomerically pure compounds (XI) and (XII). By contrast, the single enantiomer of compound (IX) forms a chain type unlike those in any of racemic compounds (I)–(VIII), or in the enantiomerically pure compounds (XI) and

(XII), while in the racemic hemihydrate (X), where the organic component is the same as in (IX), the N—H⋯O and O—H⋯O hydrogen bonds between the organic molecules form a sheet structure unlike any other compound in this series.

For compounds (I)–(VII), the O⋯O distances in the O—H⋯O hydrogen bonds are all very similar (Table 1), as are the N⋯O distances in the N—H⋯O hydrogen bonds in (II)–(VII). However, wide variations occur across this series in the $D⋯A$ distances of the weaker interactions, suggesting that many of these may be adventitious contacts rather than significant structure builders.

Experimental

Samples of compounds (I)–(VII) were prepared following a reported general procedure using piperidine as the catalytic base (Kusanur *et al.*, 2004). Yellow–brown crystals suitable for single-crystal X-ray diffraction were grown by slow evaporation, at ambient temperature and in air, of solutions in a mixture of ethanol and dimethylformamide (1:1 *v/v*).

Analyses: for (I), yield 40%, m.p. 423–425 K (decomposition) (literature value 442–445 K; Lindwall & Maclennan, 1932); MS (EI) *m/z* (% abundance): 249 (6), 222 (100), 119 (41), 105 (86). For (II), yield 43%, m.p. 458 K (decomposition) (literature value 458–460 K; Lindwall & Maclennan, 1932); MS (EI) *m/z* (% abundance): 281 [*M*$^+$] (1), 263 (3), 236 (34), 119 (100). For (III), yield 46%, m.p. 489–491 K (decomposition); MS (EI) *m/z* (% abundance): 285 [*M*$^+$] (2), 267 (3), 240 (40), 123 (100), 119 (41). For (IV), yield 60%, m.p. 465–467 K (decomposition) (literature value 470–472 K; Popp & Donigan, 1979); MS (EI) *m/z* (% abundance): 303 [*M* + 2] (0.6), 301 [*M*$^+$] (1.4), 285 (1.2), 283 (2.5), 258 (15), 256 (40), 141 (32), 139 (100), 119 (57). For (V), yield 55%, m.p. 462–464 K (decomposition) (literature value 448–453 K; Lindwall & Maclennan, 1932); MS (EI) *m/z* (% abundance): 347 [*M* + 2] (1.1), 345 [*M*$^+$] (1.0), 230 (1), 228 (1), 302 (31), 300 (32), 185 (100), 183 (98), 119 (95). For (VI), yield 45%, m.p. 449–451 K (decomposition) (literature value 458–460 K; Popp & Donigan,

organic compounds

1979); MS (EI) m/z (% abundance): 312 [M^+] (1.0), 294 (5.6), 267 (6.0), 150 (100), 119 (54). For (VII), yield 39%, m.p. 476–478 K (decomposition); MS (EI) m/z (% abundance): 273 [M^+] (1), 255 (4), 228 (34), 119 (51).

Compound (I)

Crystal data

$C_{16}H_{13}NO_3$
$M_r = 267.27$
Monoclinic, $P2_1/c$
$a = 13.876$ (3) Å
$b = 5.7725$ (8) Å
$c = 16.280$ (3) Å
$\beta = 107.799$ (16)°

$V = 1241.6$ (4) Å^3
$Z = 4$
Mo $K\alpha$ radiation
$\mu = 0.10$ mm^{-1}
$T = 120$ K
$0.26 \times 0.23 \times 0.18$ mm

Data collection

Bruker–Nonius KappaCCD area-detector diffractometer
Absorption correction: multi-scan (*SADABS*; Sheldrick, 2003)
$T_{min} = 0.975$, $T_{max} = 0.982$

15921 measured reflections
2427 independent reflections
1903 reflections with $I > 2\sigma(I)$
$R_{int} = 0.050$

Refinement

$R[F^2 > 2\sigma(F^2)] = 0.057$
$wR(F^2) = 0.144$
$S = 1.20$
2427 reflections

181 parameters
H-atom parameters constrained
$\Delta\rho_{max} = 0.25$ e Å^{-3}
$\Delta\rho_{min} = -0.29$ e Å^{-3}

Compound (II)

Crystal data

$C_{17}H_{15}NO_3$
$M_r = 281.30$
Triclinic, $P\bar{1}$
$a = 6.873$ (2) Å
$b = 7.6700$ (17) Å
$c = 13.394$ (5) Å
$\alpha = 99.48$ (2)°
$\beta = 101.68$ (3)°

$\gamma = 96.33$ (2)°
$V = 674.4$ (4) Å^3
$Z = 2$
Mo $K\alpha$ radiation
$\mu = 0.10$ mm^{-1}
$T = 120$ K
$0.34 \times 0.21 \times 0.09$ mm

Data collection

Bruker–Nonius KappaCCD area-detector diffractometer
Absorption correction: multi-scan (*SADABS*; Sheldrick, 2003)
$T_{min} = 0.968$, $T_{max} = 0.992$

15497 measured reflections
2520 independent reflections
1783 reflections with $I > 2\sigma(I)$
$R_{int} = 0.088$

Refinement

$R[F^2 > 2\sigma(F^2)] = 0.062$
$wR(F^2) = 0.159$
$S = 1.05$
2520 reflections

191 parameters
H-atom parameters constrained
$\Delta\rho_{max} = 0.33$ e Å^{-3}
$\Delta\rho_{min} = -0.28$ e Å^{-3}

Compound (III)

Crystal data

$C_{16}H_{12}FNO_3$
$M_r = 285.27$
Triclinic, $P\bar{1}$
$a = 6.8858$ (7) Å
$b = 7.7074$ (8) Å
$c = 12.7010$ (9) Å
$\alpha = 98.229$ (7)°
$\beta = 103.667$ (7)°

$\gamma = 96.034$ (9)°
$V = 641.43$ (10) Å^3
$Z = 2$
Mo $K\alpha$ radiation
$\mu = 0.11$ mm^{-1}
$T = 120$ K
$0.57 \times 0.32 \times 0.20$ mm

Data collection

Bruker–Nonius KappaCCD area-detector diffractometer
Absorption correction: multi-scan (*SADABS*; Sheldrick, 2003)
$T_{min} = 0.939$, $T_{max} = 0.978$

15674 measured reflections
2528 independent reflections
1664 reflections with $I > 2\sigma(I)$
$R_{int} = 0.054$

Refinement

$R[F^2 > 2\sigma(F^2)] = 0.053$
$wR(F^2) = 0.151$
$S = 1.11$
2528 reflections

190 parameters
H-atom parameters constrained
$\Delta\rho_{max} = 0.29$ e Å^{-3}
$\Delta\rho_{min} = -0.33$ e Å^{-3}

Compound (IV)

Crystal data

$C_{16}H_{12}ClNO_3$
$M_r = 301.72$
Triclinic, $P\bar{1}$
$a = 6.987$ (2) Å
$b = 7.689$ (4) Å
$c = 12.907$ (4) Å
$\alpha = 99.30$ (3)°
$\beta = 101.82$ (4)°

$\gamma = 96.33$ (3)°
$V = 662.4$ (5) Å^3
$Z = 2$
Mo $K\alpha$ radiation
$\mu = 0.30$ mm^{-1}
$T = 120$ K
$0.34 \times 0.22 \times 0.10$ mm

Data collection

Bruker–Nonius KappaCCD area-detector diffractometer
Absorption correction: multi-scan (*SADABS*; Sheldrick, 2003)
$T_{min} = 0.920$, $T_{max} = 0.971$

2604 measured reflections
2604 independent reflections
2051 reflections with $I > 2\sigma(I)$

Refinement

$R[F^2 > 2\sigma(F^2)] = 0.043$
$wR(F^2) = 0.114$
$S = 1.07$
2604 reflections

191 parameters
H-atom parameters constrained
$\Delta\rho_{max} = 0.25$ e Å^{-3}
$\Delta\rho_{min} = -0.40$ e Å^{-3}

Table 1
Hydrogen bonds and short intermolecular contacts (Å, °) for compounds (I)–(VII).

$Cg1$ represents the centroid of the C3a/C4–C7/C7a ring.

Compound	$D—H\cdots A$	$D—H$	$H\cdots A$	$D\cdots A$	$D—H\cdots A$
(I)	N1—H1$\cdots$O3^i	0.88	2.15	2.918 (3)	146
	O3—H3$\cdots$O2^{ii}	0.82	1.97	2.762 (3)	163
(II)	N1—H1$\cdots$O2^{iii}	0.88	1.99	2.838 (3)	162
	O3—H3$\cdots$O2^{ii}	0.84	1.90	2.729 (3)	169
(III)	N1—H1$\cdots$O2^{iii}	0.88	1.99	2.842 (2)	163
	O3—H3$\cdots$O2^{ii}	0.82	1.93	2.746 (2)	172
	C325—H325$\cdots$$Cg1^{iv}$	0.95	2.69	3.614 (3)	164
(IV)	N1—H1$\cdots$O2^{iii}	0.88	2.00	2.843 (3)	160
	O3—H3$\cdots$O2^{ii}	0.87	1.88	2.752 (3)	174
	C31—H31$B\cdots$O2^{ii}	0.99	2.50	3.276 (3)	135
	C323—H323$\cdots$O32^v	0.95	2.51	3.281 (4)	138
	C325—H325$\cdots$$Cg1^{iv}$	0.95	2.97	3.890 (3)	164
(V)	N1—H1$\cdots$O2^{iii}	0.88	2.01	2.851 (4)	160
	O3—H3$\cdots$O2^{ii}	0.86	1.90	2.746 (4)	167
	C31—H31$B\cdots$O2^{ii}	0.99	2.49	3.257 (4)	134
	C323—H323$\cdots$O32^v	0.95	2.49	3.271 (4)	140
(VI)	N1—H1$\cdots$O2^{iii}	0.88	1.99	2.848 (3)	164
	O3—H3$\cdots$O2^{ii}	0.86	1.90	2.756 (4)	175
	C31—H31$B\cdots$O2^{ii}	0.99	2.55	3.330 (4)	135
	C323—H323$\cdots$O32^v	0.95	2.52	3.308 (4)	140
	C326—H326$\cdots$O33^{vi}	0.95	2.49	3.304 (4)	143
(VII)	N1—H1$\cdots$O2^{vii}	0.88	2.00	2.843 (3)	160
	O3—H3$\cdots$O2^{ii}	0.82	1.96	2.736 (2)	158
	C7—H7$\cdots$O3^v	0.95	2.58	3.443 (3)	151
	C31—H31$B\cdots$O2^{ii}	0.99	2.59	3.382 (3)	137

Symmetry codes: (i) x, $-1 + y$, z; (ii) $1 - x$, $1 - y$, $1 - z$; (iii) $-x$, $1 - y$, $1 - z$; (iv) $1 - x$, $1 - y$, $2 - z$; (v) $1 + x$, y, z; (vi) $-1 + x$, y, z; (vii) $2 - x$, $1 - y$, $1 - z$.

Table 2
Parameters (Å) for interactions between the substituted aryl rings (C321–C326) in the molecules at (x, y, z) and $(2 - x, 1 - y, 1 - z)$ in compounds (II)–(VI).

D_1 is the interplanar spacing, D_2 the ring-centroid separation and D_3 the ring-centroid offset (slippage).

Compound	D_1	D_2	D_3
(II)	3.553 (2)	3.820 (2)	1.403 (2)
(III)	3.421 (2)	3.704 (2)	1.420 (2)
(IV)	3.435 (2)	3.708 (2)	1.396 (2)
(V)	3.490 (3)	3.739 (3)	1.342 (3)
(VI)	3.408 (2)	3.691 (2)	1.417 (2)

Compound (V)

Crystal data

$C_{16}H_{12}BrNO_3$
$M_r = 346.18$
Triclinic, $P\bar{1}$
$a = 7.016 (3)$ Å
$b = 7.7349 (12)$ Å
$c = 13.052 (6)$ Å
$\alpha = 99.69 (3)°$
$\beta = 101.51 (4)°$

$\gamma = 96.70 (3)°$
$V = 675.8 (4)$ Å^3
$Z = 2$
Mo $K\alpha$ radiation
$\mu = 3.05$ mm^{-1}
$T = 120$ K
$0.46 \times 0.25 \times 0.22$ mm

Data collection

Bruker–Nonius KappaCCD area-detector diffractometer
Absorption correction: multi-scan (*SADABS*; Sheldrick, 2003)
$T_{min} = 0.385$, $T_{max} = 0.553$

18834 measured reflections
2800 independent reflections
2215 reflections with $I > 2\sigma(I)$
$R_{int} = 0.075$

Refinement

$R[F^2 > 2\sigma(F^2)] = 0.040$
$wR(F^2) = 0.087$
$S = 1.09$
2800 reflections

190 parameters
H-atom parameters constrained
$\Delta\rho_{max} = 0.57$ e Å^{-3}
$\Delta\rho_{min} = -0.73$ e Å^{-3}

Compound (VI)

Crystal data

$C_{16}H_{12}N_2O_5$
$M_r = 312.28$
Triclinic, $P\bar{1}$
$a = 7.026 (1)$ Å
$b = 7.598 (3)$ Å
$c = 13.365 (4)$ Å
$\alpha = 97.54 (3)°$
$\beta = 102.67 (2)°$

$\gamma = 96.46 (2)°$
$V = 682.7 (3)$ Å^3
$Z = 2$
Mo $K\alpha$ radiation
$\mu = 0.12$ mm^{-1}
$T = 120$ K
$0.27 \times 0.17 \times 0.12$ mm

Data collection

Bruker–Nonius KappaCCD area-detector diffractometer
Absorption correction: multi-scan (*SADABS*; Sheldrick, 2003)
$T_{min} = 0.970$, $T_{max} = 0.986$

19392 measured reflections
2683 independent reflections
1528 reflections with $I > 2\sigma(I)$
$R_{int} = 0.096$

Refinement

$R[F^2 > 2\sigma(F^2)] = 0.057$
$wR(F^2) = 0.158$
$S = 1.07$
2683 reflections

208 parameters
H-atom parameters constrained
$\Delta\rho_{max} = 0.29$ e Å^{-3}
$\Delta\rho_{min} = -0.33$ e Å^{-3}

Compound (VII)

Crystal data

$C_{14}H_{11}NO_3S$
$M_r = 273.30$
Triclinic, $P\bar{1}$
$a = 6.5958 (7)$ Å
$b = 7.9577 (14)$ Å
$c = 12.045 (3)$ Å
$\alpha = 78.51 (2)°$
$\beta = 76.555 (13)°$

$\gamma = 84.559 (15)°$
$V = 601.8 (2)$ Å^3
$Z = 2$
Mo $K\alpha$ radiation
$\mu = 0.27$ mm^{-1}
$T = 120$ K
$0.41 \times 0.23 \times 0.14$ mm

Data collection

Bruker–Nonius KappaCCD area-detector diffractometer
Absorption correction: multi-scan (*SADABS*; Sheldrick, 2003)
$T_{min} = 0.885$, $T_{max} = 0.963$

14010 measured reflections
2355 independent reflections
1798 reflections with $I > 2\sigma(I)$
$R_{int} = 0.058$

Refinement

$R[F^2 > 2\sigma(F^2)] = 0.045$
$wR(F^2) = 0.113$
$S = 1.04$
2355 reflections
172 parameters

H-atom parameters constrained
$\Delta\rho_{max} = 0.31$ e Å^{-3}
$\Delta\rho_{min} = -0.31$ e Å^{-3}

All H atoms were located in difference maps. H atoms bonded to C or N atoms were then treated as riding atoms in geometrically idealized positions, with C—H = 0.95 (aromatic and thienyl), 0.98 (CH$_3$) or 0.99 Å (CH$_2$), and N—H = 0.88 Å, and with $U_{iso}(H) = kU_{eq}(C,N)$, where $k = 1.5$ for the methyl group in compound (II), which was permitted to rotate but not to tilt, and 1.2 for all other H atoms bonded to C or N atoms. H atoms bonded to O atoms were permitted to ride at the positions deduced from difference maps, with $U_{iso}(H) = 1.5U_{eq}(O)$, giving O—H distances in the range 0.82–0.87 Å (Table 1). Compound (IV) was treated as a nonmerohedral twin. A modified reflection data file was prepared using the TwinRotMat option in *PLATON* (Spek, 2009) and used with the HKLF5 option in *SHELXL* (Sheldrick, 2008), giving twin fractions of 0.269 (2) and 0.731 (2).

For all compounds, data collection: *COLLECT* (Nonius, 1999); cell refinement: *DIRAX/LSQ* (Duisenberg *et al.*, 2000); data reduction: *EVALCCD* (Duisenberg *et al.*, 2003); program(s) used to solve structure: *SIR2004* (Burla *et al.*, 2005); program(s) used to refine structure: *SHELXL97* (Sheldrick, 2008); molecular graphics: *PLATON* (Spek, 2009); software used to prepare material for publication: *SHELXL97* and *PLATON*.

organic compounds

References

Acosta, L. M., Bahsas, A., Palma, A., Cobo, J., Hursthouse, M. B. & Glidewell, C. (2009). *Acta Cryst.* C**65**, o92–o96.

Allen, F. H. (2002). *Acta Cryst.* B**58**, 380–388.

Bernstein, J., Davis, R. E., Shimoni, L. & Chang, N.-L. (1995). *Angew. Chem. Int. Ed. Engl.* **34**, 1555–1573.

Burla, M. C., Caliandro, R., Camalli, M., Carrozzini, B., Cascarano, G. L., De Caro, L., Giacovazzo, C., Polidori, G. & Spagna, R. (2005). *J. Appl. Cryst.* **38**, 381–388.

Chen, G., Liu, B., Tang, Y. & Xu, J. (2009). *Acta Cryst.* E**65**, o1723.

Duisenberg, A. J. M., Hooft, R. W. W., Schreurs, A. M. M. & Kroon, J. (2000). *J. Appl. Cryst.* **33**, 893–898.

Duisenberg, A. J. M., Kroon-Batenburg, L. M. J. & Schreurs, A. M. M. (2003). *J. Appl. Cryst.* **36**, 220–229.

Flack, H. D. (1983). *Acta Cryst.* A**39**, 876–881.

Kusanur, R. A., Ghate, M. & Kulkarni, M. V. (2004). *J. Chem. Sci.* **116**, 265–270.

Lindwall, H. G. & Maclennan, J. S. (1932). *J. Am. Chem. Soc.* **54**, 4739–4744.

Luppi, G., Cozzi, P. G., Monari, M., Kaptein, B., Broxterman, Q. B. & Tomasini, C. (2005). *J. Org. Chem.* **70**, 7418–7421.

Luppi, G., Monari, M., Corrêa, R. J., Violante, F. de A., Pinto, A. C., Kaptein, B., Broxterman, Q. B., Garden, S. J. & Tomasini, C. (2006). *Tetrahedron*, **62**, 12017–12024.

Nonius (1999). *COLLECT*. Nonius BV, Delft, The Netherlands.

Popp, F. D. & Donigan, B. E. (1979). *J. Pharm. Sci.* **68**, 519–520.

Sheldrick, G. M. (2003). *SADABS*. Version 2.10. University of Göttingen, Germany.

Sheldrick, G. M. (2008). *Acta Cryst.* A**64**, 112–122.

Spek, A. L. (2009). *Acta Cryst.* D**65**, 148–155.

Xing, X.-N., Li, L., Zhu, X.-Y. & Chen, J.-R. (2007). *Acta Cryst.* E**63**, o2969–o2970.